$CaCu_3M_4O_{12}$ indeed provides a unique opportunity to explore Kondo phenomena in transition metal compounds, where one may achieve lower Kondo temperatures by suitably varying the *M* constituent." (Reported by Ashish Chainani)

*This report features the work of Liu Hao Tjeng, Atsushi Hariki and their collaborators published in Phys. Rev. X* ***12****, 011017 (2022).*

### TPS 45A1 Submicron Soft X-ray Spectroscopy
### SP 12U1 HAXPES/Photoemission

- Hard/Soft PES, XAS
- Condensed-matter Physics

### References


1. G. R. Stewart, Rev. Mod. Phys. **56**, 755 (1984).
2. S. Kondo, D. C. Johnston, C. A. Swenson, F. Borsa, A. V. Mahajan, L. L. Miller, T. Gu, A. I. Goldman, M. B. Maple, D. A. Gajewski, E. J. Freeman, N. R. Dilley, R. P. Dickey, J. Merrin, K. Kojima, G. M. Luke, Y. J. Uemura, O. Chmaissem, J. D. Jorgensen, Phys. Rev. Lett. **78**, 3729 (1997).
3. W. Kobayashi, I. Terasaki, J.-i. Takeya, I. Tsukada, Y. Ando, J. Phys. Soc. Jpn. **73**, 2373 (2004).
4. H. Xiang, X. Liu, E. Zhao, J. Meng, Z. Wu, Phys. Rev. B **76**, 155103 (2007).
5. D. Takegami , C.-Y. Kuo, K. Kasebayashi, J.-G. Kim, C. F. Chang, C. E. Liu, C. N. Wu, D. Kasinathan, S. G. Altendorf, K. Hoefer, F. Meneghin, A. Marino, Y. F. Liao, K. D. Tsuei, C. T. Chen, K.-T. Ko, A. Günther, S. G. Ebbinghaus , J. W. Seo, D. H. Lee, G. Ryu, A. C. Komarek, S. Sugano, Y. Shimakawa, A. Tanaka, T. Mizokawa, J. Kuneš, L. H. Tjeng , A. Hariki, Phys. Rev. X **12**, 011017 (2022).


# High-Speed and Energy-Efficient Electronics

*The coexistence of a topological surface state and a Rashba surface state in a Dirac semimetal, α-Sn, may significantly enhance the potential for spintronic applications.*

The diverse topological phases of matter have been studied in detail, not only out of scientific interest, but also for their potential applications. Indicated by their special Dirac cones in the band structure, novel quantum oscillations are frequently observed in systems hosting Dirac fermions. Applications utilizing these Dirac states are now being extensively investigated in many fields, including thermoelectric devices, photonic devices, spin-based field-effect transistors, and memories, *etc*. A group IV element with a diamond structure, α-Sn is one of the materials that provides an ideal platform for realizing abundant topological phases based on its non-trivial band topology. Moreover, a large spin-to-charge conversion at room temperature has been demonstrated *via* spin pumping, while an efficient current-induced magnetization switching was achieved in α-Sn/magnetic metal heterostructures, thus making α-Sn attractive for spintronic applications.

In the exploration of topological phase transitions, bandgap engineering *via* quantum confinement effects or strain modulation has been a commonly used approach in addition to chemical doping. Band evolution in a few layers of thin films attracts great attention since the confinement effect has a significant influence on the bandgap. A thickness-dependent topological phase transition often occurs when the system undergoes a band inversion during the bandgap engineering. A single-layer α-Sn, especially in the (111) orientation, is of great interest because of its honeycomb-like structure in analogy to graphene and its large quantum-spin-Hall gap. As the film becomes thicker, a two-dimensional to three-dimensional (3D) band transition takes place and the unstrained α-Sn becomes a zero-gap semiconductor. Besides the interesting phase transition found in α-Sn(111), the band evolution in the (001) orientation is also worth studying but has yet to be fully explored in a wide thickness range.

To deepen understanding of the evolution of topological transition in α-Sn(001) for increasing thickness, Raynien Kwo (National Tsing Hua University), Cheng-Maw Cheng (NSRRC) and their teams studied the electronic structure of in-plane compressively strained α-Sn(001) on InSb(001) substrates with varying thicknesses ranging from a few bilayers (BL) to 370 BLs. Comprehensive angle-resolved photoemission spectroscopy (ARPES) experiments at **TLS 21B1** were carried out on high-quality α-Sn thin films prepared using molecular beam epitaxy (MBE). A critical thickness of 5–6 BLs for the transition between topologically trivial and non-trivial phases was experimentally determined for the first time in undoped α-Sn(001) thin films. As the film thickness exceeded 30 BLs, additional Rashba-like surface states (RSS) were newly identified and could be associated with the preformed topological surface states (TSS) in the phase transition to a 3D topological insulator (TI). Moreover, they compared with the density functional theory (DFT) calculations and found the 3D Dirac nodes at $k_z \approx 0.0276$

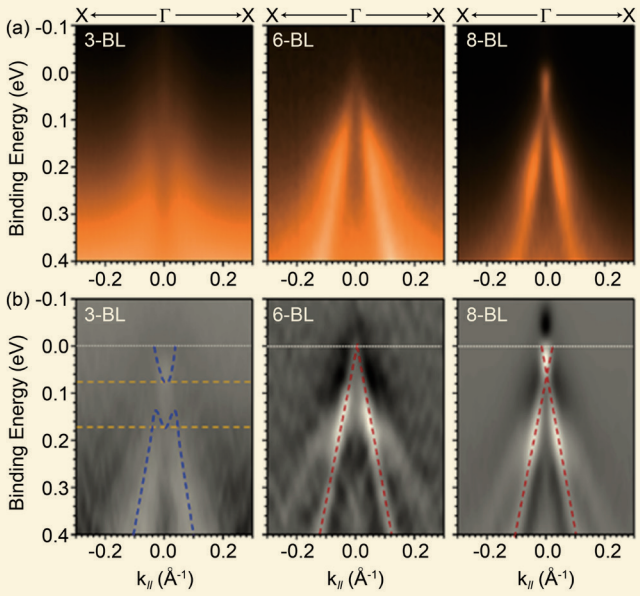


**Fig. 1**: (a) ARPES spectra of 3-, 6-, and 8-BL α-Sn(001) along $\bar{\Gamma}$–$\bar{X}$ with an incident photon energy of 21.2 eV. (b) Second-derivative plots of (a). [Reproduced from Ref. 1]

Å$^{-1}$ away from the Γ point around the Fermi energy ($E_F$). The thickness- and strain-dependent topological phase transitions in α-Sn(001) provide fruitful insights into the surface electronic structure of α-Sn and can be generalized to other Dirac materials.

The band evolution in a few BLs of α-Sn was initially discussed, focusing on the evolution of a topological surface state (TSS1). **Figure 1** displays the ARPES spectra of these few BLs (3-, 6- and 8 BLs) α-Sn samples and the corresponding second-derivative plots along $\bar{\Gamma}$–$\bar{X}$. An M-shaped hole band and a V-shaped electron pocket are observed in the 3- and 4-BL samples, and can be attributed to the wavefunction hybridization of the top and bottom surface states. The conduction band minimum was located at an ~0.07 eV binding energy ($E_B$) and the valence band maximum was at ~0.17 eV $E_B$ at $\bar{\Gamma}$. The gap size was approximately 100 meV. The separated hole and electron bands transformed into a linearly dispersive TSS1 as the films grew thicker than 6 BLs. In an 8-BL sample, sharper ARPES spectra with a gapless TSS1 were attained. The TSS1 in the 8-BL sample had the same Fermi velocity as that in a 6-BL one; the DP of TSS1 in the 8-BL sample was ~60 meV higher in $E_B$ compared to that in the 6-BL sample. This experimental observation of the critical thickness in the topological phase transition is consistent with our DFT calculations and a recent prediction for free-standing α-Sn(001).

During the survey of TSSs in α-Sn, they discovered an extra pair of surface states located outside TSS1 in all α-Sn films thicker than 30 BLs. **Figure 2(a)** displays the constant energy mappings of 370-BL α-Sn; distinct square-like intensity distributions (yellow arrows) were observed outside the Dirac cone of TSS1 (red dashed lines). A significant difference in the band structures in the $\bar{\Gamma}$–$\bar{X}$ and $\bar{\Gamma}$–$\bar{M}$ high-symmetry directions shown in **Figs. 2(b)–2(e)** is that a large band splitting of RSSs was clearly

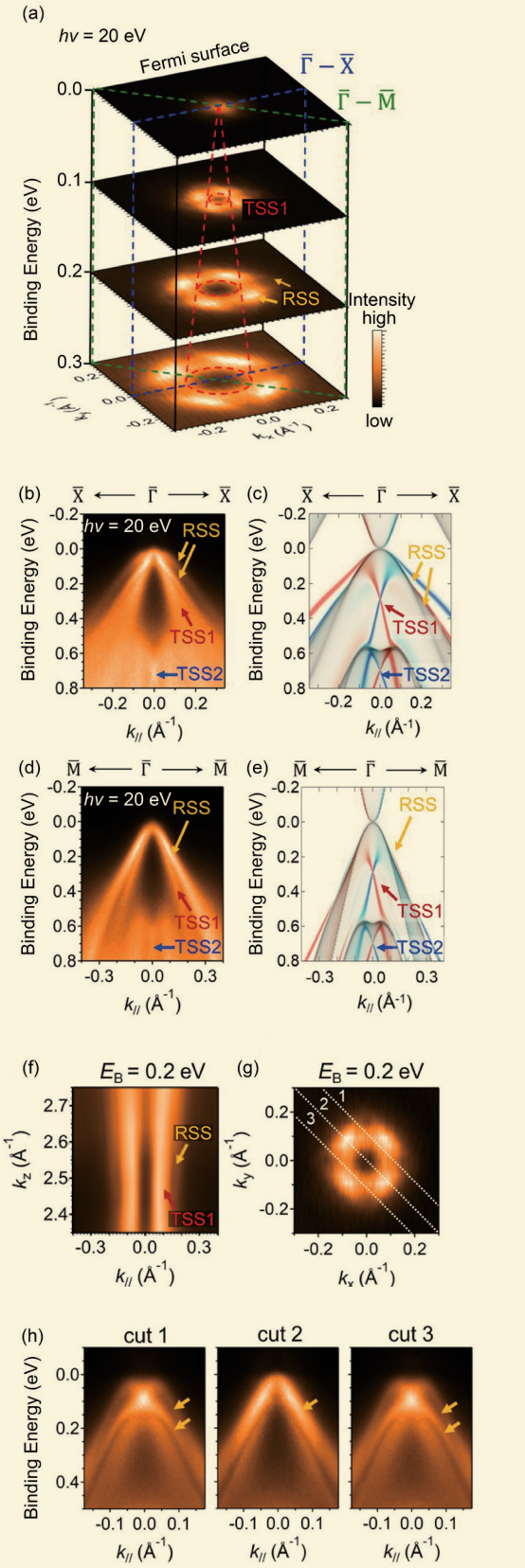


**Fig. 2**: (a) Stack of constant energy contours of 370-BL strained α-Sn(001) thin film with the TSS1 marked by red dashed lines and the RSS marked by yellow arrows. (b) ARPES spectra and (c) DFT results along $\bar{\Gamma}$–$\bar{X}$. (d) ARPES spectra and (e) DFT results along $\bar{\Gamma}$–$\bar{M}$. (f) $k_z k_{//}$ plot ($k_{//}$ along $\bar{\Gamma}$–$\bar{X}$) at 0.2 eV $E_B$. (g) Constant energy contour at 0.2 eV $E_B$. (h) ARPES spectra along $\bar{\Gamma}$–$\bar{M}$ (cut 2) and other parallel cuts (1 and 3) with an incident photon energy of 20 eV; each cut is separated by 0.078 Å$^{-1}$ with its direction labeled in (g). [Reproduced from Ref. 1]

resolved in $\bar{\Gamma}$–$\bar{X}$, whereas the band splitting of RSSs was tiny in $\bar{\Gamma}$–$\bar{M}$, suggesting anisotropic behavior of the RSSs. In their DFT calculations, spin-split surface bands (a typical characteristic of RSSs) were observed and showed excellent agreement with the experimental results. An additional Rashba spin orbital coupling (SOC) was included in the DFT calculations; without this Rashba SOC, the RSSs still existed but the band splitting in momentum was somewhat small. This anisotropic behavior of RSSs could be correlated to a warping effect caused by the crystal symmetry in α-Sn. Moreover, an estimated Rashba coefficient $\alpha_R \approx 1.5$ eV·Å is ~4.5 times larger than that of Au(111). Having RSSs coexisting with TSS1 could provide an efficient and gate-tunable spin-charge conversion, which offers great potential in the application of spintronics devices.

In summary, their work reports a comprehensive study on the electronic structure of compressively strained α-Sn/InSb(001). A transition from a topologically trivial to non-trivial phase was observed at the critical thickness of 6 BLs. A pair of RSSs was newly discovered in α-Sn films thicker than 30 BLs; they were regarded as a preformed TSS and this provided insights into the evolution of a TSS in a topological phase transition and the surface electronic structure of a Dirac material. As revealed by their results, α-Sn provides a rich playground for realizing various topological phases of matter, such as topological Dirac semimetal (TDS), TI, *etc*. The coexistence of RSSs and TSS1, as typified by an efficient and gate-tunable spin-charge conversion, may offer great opportunities for applications in the modern technology of spintronics. (Reported by Cheng-Maw Cheng)

*This report features the work of Raynien Kwo, Cheng-Maw Cheng and their collaborators published in Phys. Rev. B* ***105*** *, 075109 (2022).*

### TLS 21B1 Angle-resolved UPS

- High-resolution ARPES
- Materials Science, Condensed-matter Physics

### Reference

1. K. H. M. Chen, K. Y. Lin, S. W. Lien, S. W. Huang, C. K. Cheng, H. Y. Lin, C.-H. Hsu, T.-R. Chang, C.-M. Cheng, M. Hong, J. Kwo, Phys. Rev. B **105**, 075109 (2022).

# A Simple and Efficient Method for Hydrogen Spillover and Storage

*Atomic hydrogen spillover and storage was achieved and characterized for single-site catalysts through precise control of the coverage of Ti on graphene. This realization has potential to extend all graphitic materials to store hydrogen.*

Since the beginning of the industrial revolution in the 18th century, coal has been increasingly used as an energy source for the operation of machines, which have made human life convenient. In the 19th century, the advent of the petrochemical industry accelerated technological development. Although industrial, economical, and technological advances have made human life considerably convenient, they have come at the price of an energy crisis and environmental issues such as global warming. Furthermore, petroleum is expected to be completely exhausted in the future. Therefore, identifying alternative clean energy sources is inevitable. Hydrogen energy is one of the most notable candidates for alternative clean energy because its conversion emits no carbon and produces only water as a by-product, thereby minimizing the progress of global warming. Accordingly, technologies for effective production and storage of hydrogen are warranted.

Chung-Lin Wu (National Cheng Kung University) and Chia-Hao Chen (NSRRC), in collaboration with the National Enterprise for nanoScience and nanoTechnology (NEST, Italy), discovered a high-efficiency hydrogen storage method. In early studies, graphene was revealed to be inert when exposed to hydrogen molecules but highly active when exposed to H atoms.[1,2] In their previous works, they demonstrated that single Ti atoms can adsorb on graphene at its energetically favorable hollow sites[3] and studied the structural variation of graphene upon Ti deposition and its hydrogen uptake by conducting scanning tunneling microscopy.[4] Drawing on these previous results, they further